JAAS

ROYAL SOCIETY OF CHEMISTRY

PAPER

View Article Online
View Journal | View Issue

Cite this: J. Anal. At. Spectrom., 2023, 38, 2028

Development of a simultaneous LA-ICP-MS & LIBS method for the investigation of polymer degradation

Jakob Willner, [ab] Lukas Brunnbauer, [a] C. Derrick Quarles, Jr, [c] Michael Nelhiebel,[b] Silvia Larisegger[b] and Andreas Limbeck *[a]

This work shows the development and optimization of simultaneous 193 nm LA-ICP-MS & LIBS methods for the spatially resolved analysis of polymer thin films of polyimide, polystyrene, and polyvinylpyrrolidone, which were exposed to a UV treatment and weathered in a corrosive atmosphere containing hydrogen sulfide, to investigate polymer ageing and degradation in harsh environments. Evaluating the information from a broadband multichannel LIBS instrument enabled the spatially resolved discrimination of the used polymer types with a lateral resolution of 40 μm. At the same time, a high-resolution spectrometer with an ICCD camera could detect oxidation derived from the UV treatment, and ICP-MS data could measure differences in the sulfur uptake derived from the sample film H_2S weathering. In additional experiments, the depth resolution was optimized, depending on the polymer type to 150–360 nm, to gain information on the H_2S diffusion profile and the sample depth affected by oxidation. Matrix-matched standards were used to calibrate the ICP-MS, enabling simultaneous determination of quantitative sulfur diffusion profiles and the influence of the UV treatment on the diffusion profiles. The capabilities of the combined measurement methods based on a 193 nm laser are well demonstrated on the differently treated polymer thin film samples used in this work, revealing spatially resolved information on different oxidation behavior, different sulfur diffusion profiles, and a significant decrease of the sulfur uptake in UV treated films – information that is not accessible with setups in previous literature.

Received 17th July 2023
Accepted 31st August 2023

DOI: 10.1039/d3ja00237c

rsc.li/jaas

1. Introduction

Polymer thin films and polymer coatings are integral components in highly advanced fields, such as the microelectronics and semiconductor industry, for electrical insulation and protection of sensitive components from environmental influences.[1] This is particularly relevant in harsh environments (*e.g.*, for industrial and automotive electronics), where increased levels of corrosive gases, such as NO_x, SO_2, or H_2S, and high levels of humidity can be present,[2,3] and high thermal stress due to strong variabilities in power load may be part of the operational routine (*e.g.*, power electronics).[4] For such applications, the properties of the applied polymer must be thoroughly tuned to ensure their protection capabilities, as well as stability for a specified lifetime. This makes them a fundamental aspect of product reliability.[5] But also in other applications, the barrier characteristics against potentially harmful gaseous penetrators are essential and thoroughly investigated, *e.g.*, food or medical packaging, consumer goods, or corrosion protection of metals.[6–8] In some uses, the polymers are exposed to daylight (*i.e.*, UV-radiation), which is well known for its influences on polymer material properties.[9] However, deliberate exposure to UV radiation can also be a part of the production process (*e.g.*, photoinitiation of the polymerization reaction, cross-linking, curing).[10,11] Thus, barrier properties of polymer materials regarding the uptake of gases from the environment and the influence of UV exposure on those properties are of profound interest.

To evaluate the performance of such polymer materials for the mentioned purposes, testing equipment is required to expose the materials to controlled environmental conditions (radiation, humidity, corrosive gases, temperature), along with techniques and methods for chemical characterization that allow measurement of the uptake of gases, as well as changes in the polymer that indicate consequences of degradation. Techniques commonly used for chemical analysis of polymers and polymer degradation are FTIR spectroscopy, Raman spectroscopy, or MALDI-ToF-MS.[12–16] While these techniques can measure lateral distributions and offer information on a molecular level (*i.e.*, the presence or absence of certain bonds and molecular fragments), they cannot provide depth-resolved analysis. Furthermore, no inherent

[a]TU Wien, Institute of Chemical Technologies and Analytics, Getreidemarkt 9/164-I2AC, 1060 Vienna, Austria. E-mail: andreas.limbeck@tuwien.ac.at

[b]KAI Kompetenzzentrum Automobil-und Industrieelektronik GmbH, Technologiepark Villach – Europastraße 8, 8524 Villach, Austria

[c]Elemental Scientific, Inc., 7277 World Communications Dr., Omaha, NE, USA

elemental information is received, and in addition, these techniques lack sensitivity to determine the uptake of gases on a μg g^{-1} level.

Laser ablation-inductively coupled plasma-mass spectrometry (LA-ICP-MS) and laser-induced breakdown spectroscopy (LIBS) are powerful techniques for spatially resolved elemental analysis. While LA-ICP-MS offers better sensitivity down to the ng g^{-1} level, some of the main constituents of polymers (H, O, N) are not possible to measure since the ICP is an atmospheric plasma. However, LIBS can measure these elements when the sample is in an inert atmosphere (*e.g.*, Ar or He gas). Furthermore, LIBS can measure emissions from molecular species (*e.g.*, CN, C_2), which can be evaluated for polymer discrimination and classification, or as indicators for changes in the polymer's properties (*i.e.*, degradation).[17–20] Since both techniques are initiated by a focused laser pulse on the sample surface, they can be merged into a combined measurement method, simultaneously acquiring the characteristic information of both techniques originating from the same sample location.

While this LA-ICP-MS & LIBS combination has already been published several times for various applications (*e.g.*, for geochemical applications, elemental and discrimination analysis of coal, metal analysis in polymers),[21–24] the optimization and application for investigating polymer properties or degradation is limited. Brunnbauer *et al.* published such work in 2019, showing the capability of the combined LA-ICP-MS & LIBS approach for the analysis of polymer behavior in corrosive and degradative conditions.[25] However, the applied 266 nm Nd:YAG laser is limited in achievable ablation rate and, thereby, depth resolution, as well as its generated crater shapes derived from a Gaussian beam profile being less defined and even, compared to 193 nm ns lasers. Therefore, improvements to the published literature are required for polymer analysis, enabling discrimination of polymer types and potential classification, and spatially resolved determination of degradation effects and gas uptake, specifically in thin films.

In this work, combined (simultaneous) LA-ICP-MS & LIBS methods are developed for spatially resolved investigation of polymer degradation and gas uptake with improved spatial resolution and sensitivity, using a 193 nm ns ArF excimer laser ablation system. Improvements to the spatial resolution are enabled by the systems flat-top beam energy profile, the possible use of rectangular apertures and the improved performance of the next generation sample stage. Much higher operable repetition rates of up to 500 Hz enable improved sensitivity in ICP-MS coupling and fast measurement of large sample areas while maintaining high spatial resolution. The setup was optimized for two applications: first, the laterally resolved polymer discrimination and determination of differences in the effects of UV radiation and the consequences of the sulfur uptake in weathering experiments on thin films of different polymer types (polyimide, polystyrene, and polyvinylpyrrolidone). Secondly, for the depth-resolved determination of degradation effects derived from UV radiation together with the quantitative determination of the sulfur uptake derived from weathering experiments.

2. Experimental

2.1. Preparation of polymer films

Purchased granulates/powders of P84® polyimide (PI, Ensinger Sintimid GmbH), polystyrene (PS, Fisher Scientific), polyvinylpyrrolidone (PVP, K85-95, Acros Organics) were dissolved in *N*-methyl-2-pyrrolidon (NMP, > 99.5%, Sigma-Aldrich). The mass fraction of each polymer type in the respective solution was optimized for its viscosity and surface tension to allow a reproducible preparation of polymer films with a controlled thickness. This resulted in the use of solutions containing 10 wt% for PI, 20 wt% for PS, and 8 wt% for PVP in NMP. All sample intake and dilution steps were performed gravimetrically. 10 μL of the respective polymer solution was pipetted and evenly distributed on 10 × 10 mm^2 pieces of high-purity silicon wafers from Infineon Technologies (Villach, Austria) that were preheated to 80 °C on a hot plate. 30 minutes after application of the polymer solution, the hot plate temperature was increased to 120 °C to evaporate the remaining solvent. After another 30 minutes, the wafer pieces with the remaining polymer films were removed from the hot plate, cooled to room temperature, and stored in sealed plastic boxes at room temperature until further experiments. Additionally, samples containing all three mentioned polymer types adjacent to each other were prepared on a single silicon platelet. Those were prepared analogously using 3.3 μL of each polymer solution. The solutions were sequentially applied to a wafer piece with a pipette, each covering approximately one-third of the surface area.

For LA-ICP-MS calibration, matrix-matched standards were prepared by spiking the polymer solutions with the respective amounts of 2,2′-dithio-dipyridine (Sigma-Aldrich, ≥ 99%) and following with an identical film preparation procedure to receive standards containing sulfur in the range of 20–5000 μg g^{-1}.

2.2. UV exposure of polymer films

The UV exposure of the samples was performed under ambient atmosphere and room temperature. The samples were placed in a steel box equipped with an 11 W UV source (mercury vapor lamp, Philips PL-S 11W – UV-C), which is normally used for the observation of thin layer chromatograms, at a distance of 10 cm to the source. The PI, PS, and PVP films, as well as the samples containing all three polymer types, were exposed non-stop for 30 days. After the UV exposure, the samples were stored in sealed plastic boxes at room temperature until the weathering experiment with H_2S exposure.

2.3. Weathering experiments

The exposure of the polymer films to corrosive gases at a defined temperature and relative humidity (r.h.) was performed in an in-house developed mixed-flowing gas (MFG) setup. The test gas (1000 ppm H_2S, (v/v)) is mixed with synthetic air to the desired concentration using mass flow controllers. The relative humidity is adjusted by mixing a dry (0% r.h.) with a humidified (100% r.h.) synthetic air stream. The set gas mixture enters

a weathering cell positioned inside a laboratory oven for temperature adjustment. The samples were weathered for 48 hours using 150 ppm (v/v) H_2S at 20 °C and 85% relative humidity with a total gas flow rate of 100 mL min^{-1}, resulting in an exchange rate of 4 times the volume of the weathering cell per hour. The weathering experiment was carried out with untreated PI, PS, and PVP films, as well as with the UV-treated polymer films. To avoid potential changes during sample storage, the samples were measured immediately after the weathering experiment.

2.4. Simultaneous LA-ICP-MS & LIBS measurements

The simultaneous acquisition of LA-ICP-MS and LIBS data was performed with an "imageGEO193^{LIBS}" laser ablation system from Elemental Scientific Lasers (Bozeman, MT, USA) operating at a wavelength of 193 nm, with a "TwoVol3" ablation chamber and two fiber mounts capable of collecting the light that is emitted from the laser-induced plasma. The instrument was coupled to an "iCap Qc" ICP-MS system from Thermo Fisher Scientific (Bremen, Germany), using PTFE tubing and a "Dual Concentric Injector" (DCI) interface (ESL, Bozeman, MT, USA) with a helium flow rate of 800 mL min^{-1}. Using optical fibers, the system was further coupled to an "ESLumen" 5-channel Czerny–Turner spectrometer with CMOS detectors (ESL, Bozeman, MT, USA) for broadband LIBS spectra acquisition from 188–1097 nm with a spectral resolution of 0.1 nm, and a "Spectra HRS-750Pro" spectrometer equipped with a "PI-MAX-4" ICCD camera, both from Teledyne Princeton Instruments (Acton, MA, USA). To measure the oxygen emission (triplet @ 777.3 nm), the ICCD spectrometer was operated with an entrance-slit width of 300 μm and an 1800 g mm^{-1} grating set to a center wavelength of 777 nm, providing a spectral resolution of 0.05 nm. The spectra were recorded with a gate delay of 0.2 μs, a gate width of 10 μs, and an intensifier gain of 20. The broadband LIBS spectra were recorded using a gate delay of 0.1 μs and a gate width of 3 ms. The instrument parameters of the laser ablation system were optimized differently to meet the specific requirements for the imaging and the depth profile measurements (Table 1). The repetition rate and scan speed in the imaging experiments resulted in 50% overlapping shots (40 μm) to improve the spatial resolution.[26,27] To set the same overlap in the other spatial dimension, a line distance of 40 μm was chosen. The ICP-MS instrument was tuned daily for a maximum ^{115}In signal while ablating NIST SRM 612. The measurements of ^{34}S and ^{13}C (dwell times of 10 ms per isotope) were performed using a plasma power of 1400 W, auxiliary gas flow of 0.8 L min^{-1} argon, make-up gas of 0.8 L min^{-1} argon, and cooling gas of 13.8 L min^{-1} argon.

The laser ablation system control as well as the broadband LIBS data acquisition were performed with the software "ActiveView2" (version 1.5.0.36, ESL). The ICCD-LIBS data were acquired with "LightField®" (version 6.13, Teledyne Princeton Instruments) and the ICP-MS data with "Qtegra™" (version 2.10.3324.62, Thermo Fisher Scientific). A more detailed description of the measurements and data evaluation will be given in the respective parts of the Results and Discussion section.

3. Results and discussion

3.1. Experimental procedure

In this work, the methodology for investigating the properties of thin films of three different polymer types (PS, PI, PVP) in harsh environments was developed. Untreated and UV-treated samples were weathered in an H_2S-containing atmosphere to assess differences in the sulfur uptake behavior depending on the polymer type and the UV treatment. To enable distinction of the polymers and to identify degradation-specific changes of the polymer films caused by the UV treatment, LIBS was employed to measure the main elements carbon, oxygen, and hydrogen, as well as diatomic species C_2 and CN. Those are, except for carbon, not accessible to ICP-MS. A multichannel broadband spectrometer with CMOS detectors was used for the simultaneous acquisition of the mentioned emission lines, allowing the distinction of different polymers through chemometric evaluation of polymer-specific signals. Additionally, a high-resolution spectrometer with an ICCD detector was used for highly sensitive detection of the oxygen emission to determine the potential oxidation of the polymers through the UV treatment in the ambient atmosphere. Employment of LA-ICP-MS enables the determination of the sulfur uptake, which diffuses into the polymers as H_2S from the atmosphere, while the sensitivity of LIBS is not sufficient to determine sulfur in a μg g^{-1} concentration range with respect to the mentioned requirements for spatial resolution. Since the sulfur uptake derived from sample weathering and changes in the polymer

Table 1 Experimental parameters of the laser ablation instrument

Experiment	Imaging	Depth profiling
Pattern	Image raster (9 × 9 mm^2)	Line scan (8 mm)
Spot size	80 × 80 $μm^2$ (square shape)[a]	150 × 50 $μm^2$ (rectangular shape)[b]
Sample fluence	6 J cm^{-2}	1 J cm^{-2}
Repetition rate	50 Hz	100 Hz
Scan speed	2 mm s^{-1}	5 mm s^{-1}
Overlap	40 μm	0 μm

[a] The side of the squared spot was oriented parallel to the scan direction of the line scans. [b] The 50 μm side of the rectangular spot was oriented parallel to the scan direction of the line scans.

composition and structure from UV exposure are expected to show variations with the sample depth, the applied methods were developed and optimized to enable spatially resolved analysis using a 193 nm ArF excimer laser in a combined LA-ICP-MS/LIBS setup. Qualitative images were measured of structured polymer film samples that contain all three polymer types. This was done using high laser energy, thus delivering single-shot spectra with sufficient signal-to-noise ratio for evaluation with both LIBS detectors. To measure depth profiles with an optimized depth resolution, each polymer type was investigated using a separate sample film that contains only the respective polymer type and using a low laser fluence for the measurement, thus minimizing ablation depth per laser pulse. Additional, for these measurements, matrix-matched standards were used for LA-ICP-MS calibration to obtain quantitative depth profiles for sulfur. Fig. 1 shows a schematic depiction of the experimental procedure, showing the used sample types, the applied sample treatments, and performed analyses.

3.2. Simultaneous LA-ICP-MS & LIBS measurements

3.2.1. Imaging of multi-polymer samples. The data originating from the ICP-MS and from the broadband-LIBS were background corrected and integrated using the software "Iolite®" (version 4.8.2, ESL). The resulting pixel matrices were exported and subsequently imported together with the ICCD-LIBS data and microscopic images of the samples into the software "ImageLab" (version 4.21, Epina GmbH). ImageLab was used to align the image data and build a multimodal data cube containing the ICP-MS and LIBS data from both systems, further allowing image processing and chemometric analysis of the combined dataset. Table 2 shows the integration ranges of the evaluated LIBS emission signals. The broadband LIBS spectra and magnified areas of the evaluated signals of untreated PI, PS, and PVP are shown in Fig. 2.

Fig. 3 shows a microscopic image which was recorded before the measurement and qualitative images of a non-UV-treated and subsequently weathered multi-polymer sample for C, C_2, CN, H, and O (broadband LIBS), O (ICCD-LIBS), and ^{34}S (ICP-MS). The measured area and polymer assignments can be seen in the microscopic image (top left), the scale bar (bottom left) and color scale (bottom center) refer to the LIBS and ICP-MS images. Two small bubbles can be seen in the microscopic image. However, since no effect in the LIBS and ICP-MS images was observed, it can be assumed that they were located below the measured sample layer. Variations in the intensities for some of the single spectral descriptors (*i.e.* integrated emission line, molecular band, or ^{34}S intensity, respectively) already indicate distinctiveness between the three investigated polymer types. However, for some descriptors (CN, H, O

Table 2 LIBS emission signals and integration ranges used for evaluation

Emission signal	Integration wavelength range [nm]
C(I)	247.4–248.3
C_2 $\Delta\nu$ 0	513.7–517.7
CN	387.4–388.6
H(I)	651.7–661.5
O(I)	776.1–778.4

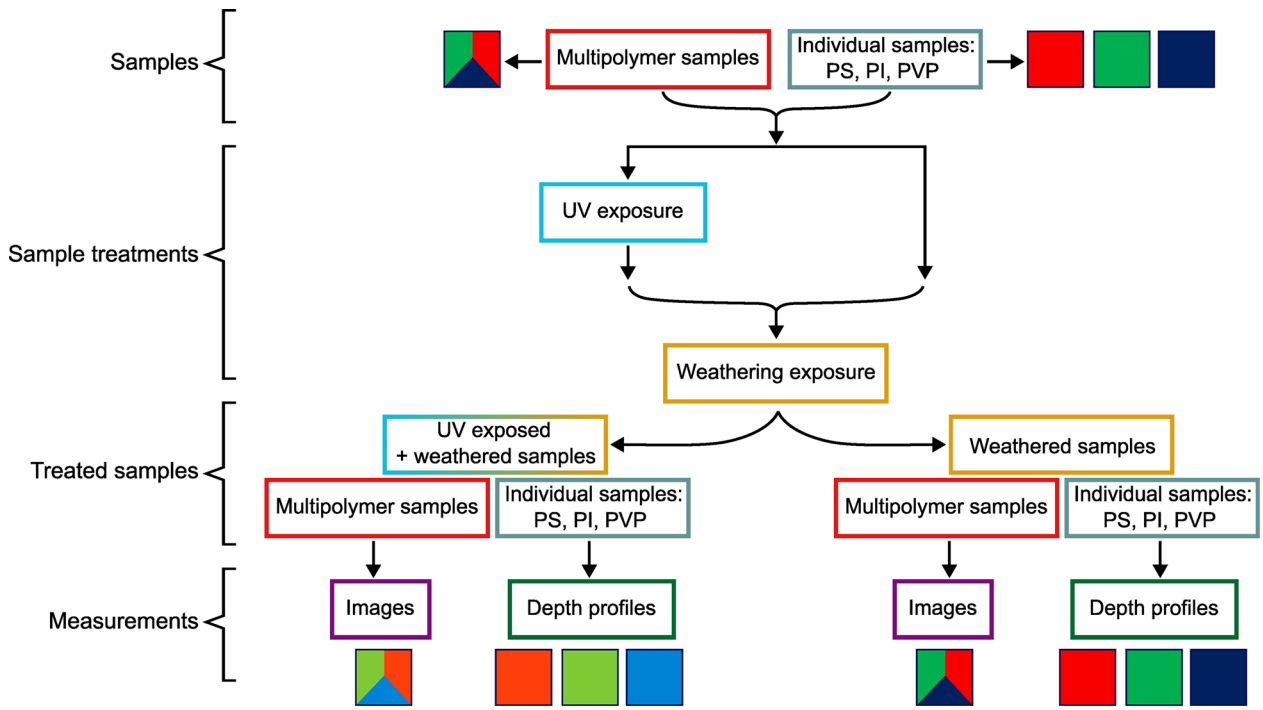

Fig. 1 Schematic depiction of the used sample types, treatments, and analyses performed.

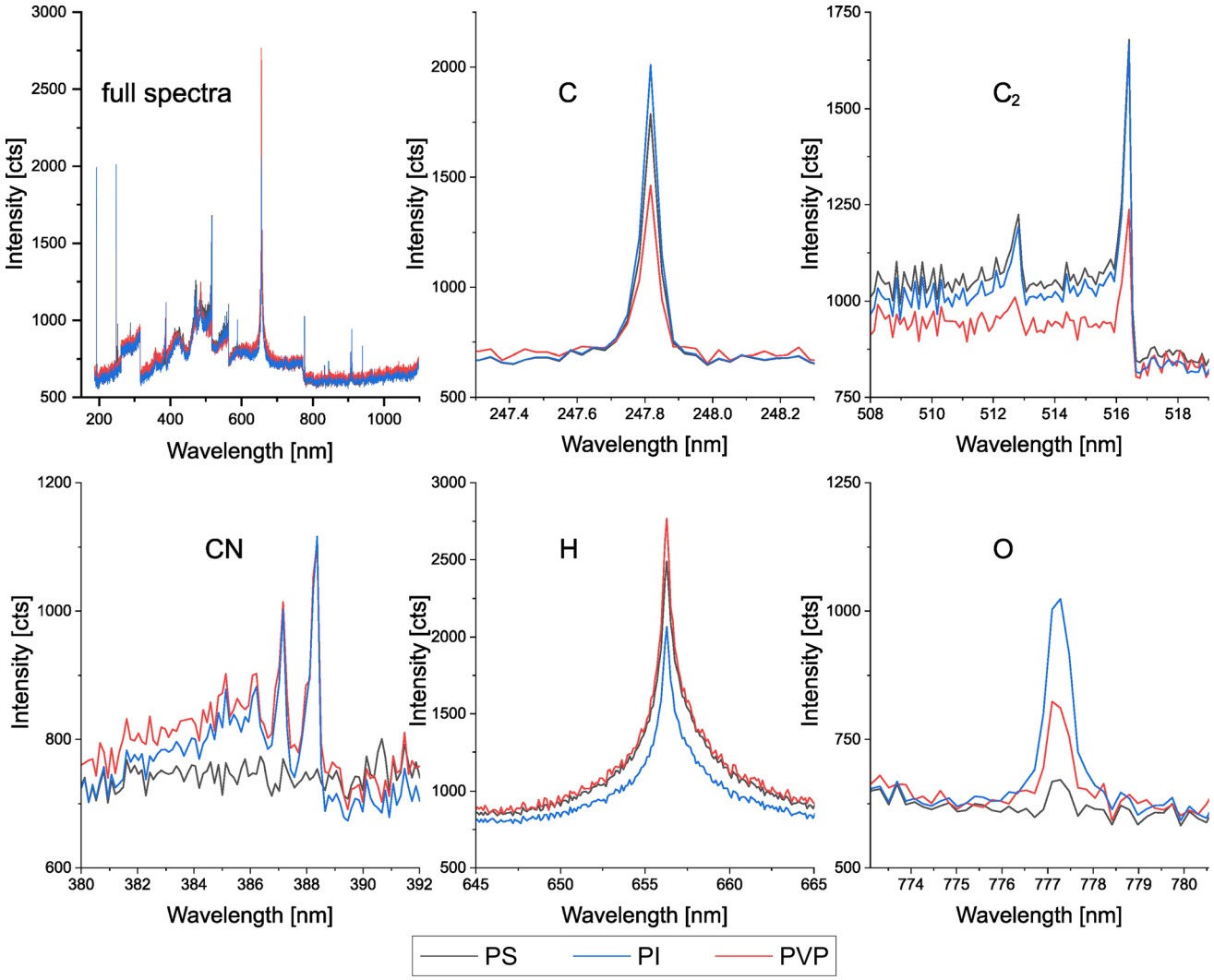

Fig. 2 Broadband LIBS spectra and magnified signals of evaluated emissions of untreated PI, PS, and PVP. 20 spectra were averaged, and instrumental parameters were used analogously to the imaging experiments.

broadband), at least two of the polymer types cannot be discriminated satisfyingly. Further, regarding a discrimination between the three polymer types using single spectral descriptors pixel-wise, the outcome would be hampered by the present noise. Using multivariate chemometric evaluation can therefore improve the distinguishability considerably.

The standardized LIBS data was used for a *k*-means cluster analysis, and the data points (*i.e.*, pixels of the image) in each of the three resulting clusters were attributed a different color (PI: green, PS: red, PVP: blue). A Principal Component Analysis (PCA) was performed with the same data to visualize the contribution of the different spectral descriptors to the discrimination result. The data points of the PCA are colored using the pixel attributes derived from the *k*-means cluster analysis. Fig. 4 shows the resulting cluster image of the *k*-means cluster analysis using the respective color code, the Bi-plot of the PCA showing the contribution of the different spectral descriptors to the principal components 1 and 2 with a good cluster separation and minimal overlap, and a very satisfactory fit of the cluster image's transparent overlay with a microscopic sample image (see Fig. 3). The cluster image contains a very low amount of wrongly assigned pixels, which further are primarily located at the interfaces between the different polymer types. The presented results demonstrate that with the developed method, polymer discrimination can be performed using single-shot spectra combined with chemometric data treatment (*k*-means, PCA) with a spatial resolution of 40 μm.

While polymer classification using LIBS combined with chemometric data evaluation is already described in literature numerous times, it is typically performed as bulk analysis by averaging or accumulating a large number of spectra for each data point to improve signal-to-noise ratios. Additionally, such work has only been reported using higher wavelengths (*e.g.*, 266 nm, 532 nm, 1064 nm),[28] which typically have much higher pulse energy than the applied 193 nm laser. Additionally, higher wavelengths are typically accompanied by much higher ablation rates, crater depths, and less defined and even crater shapes. Especially for further pushing the spatial resolution (laterally

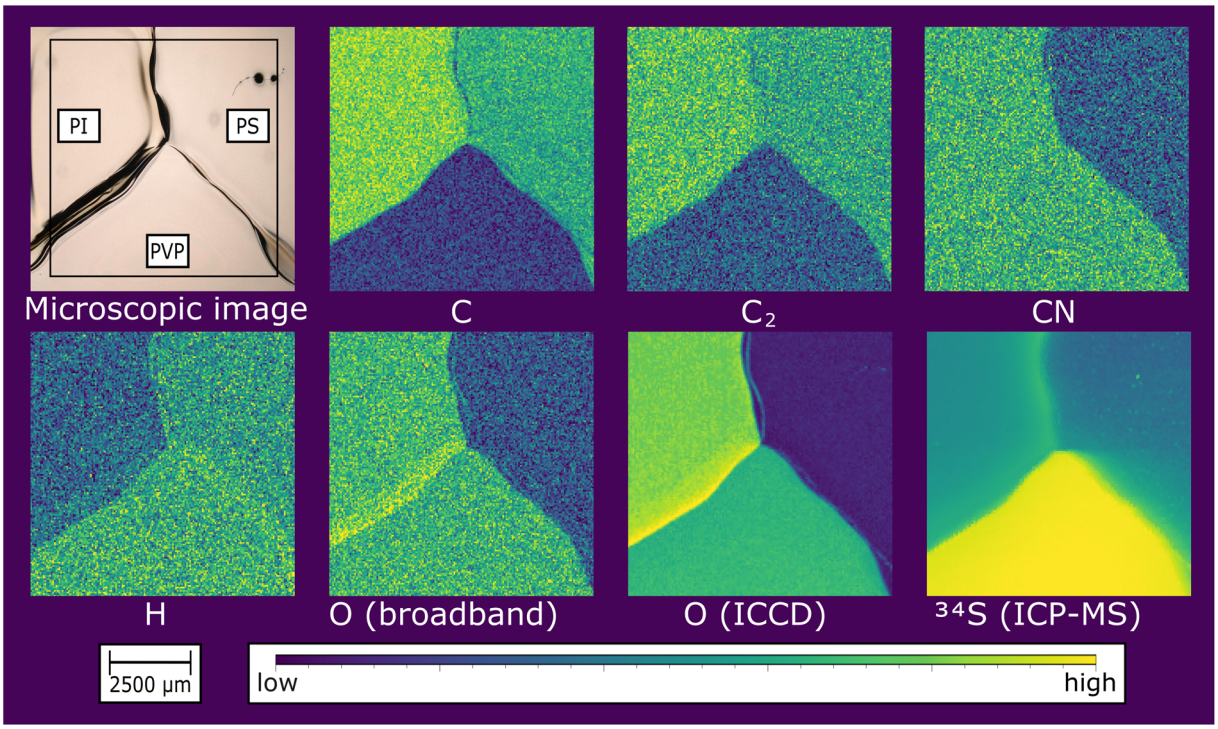

Fig. 3 Microscopic, LIBS and ICP-MS images of a non-UV-treated, weathered multi-polymer film sample containing PI, PS, and PVP.

and in depth) for the analysis of thin films, the applied 193 nm system offers more favorable ablation properties while additionally being better suited for simultaneous LA-ICP-MS measurement in terms of the formed particle aerosol. The only published work showing a spatially resolved polymer classification using LIBS was published by Brunnbauer *et al.* in 2020, using a 266 nm Nd:YAG laser and evaluating single-shot spectra recorded with a repetition rate of 10 Hz and 100 µm lateral resolution.[29] In the present work, a repetition rate of 50 Hz was used, enabling faster imaging experiments, and the lateral resolution was improved to 40 µm. To the authors' knowledge, the work presented is the first to show a spatially resolved polymer discrimination using LIBS data acquired with a 193 nm laser.

The broadband spectra of the UV-treated multi-polymer sample do not show significant differences from the untreated one. However, significant differences could be measured in the oxygen signals recorded with the ICCD detector. Fig. 5 shows histograms of the oxygen signals recorded with the ICCD detector and the sulfur signals recorded *via* ICP-MS of the images of a weathered multi-polymer sample with and without prior UV treatment. The oxygen signals of the non-

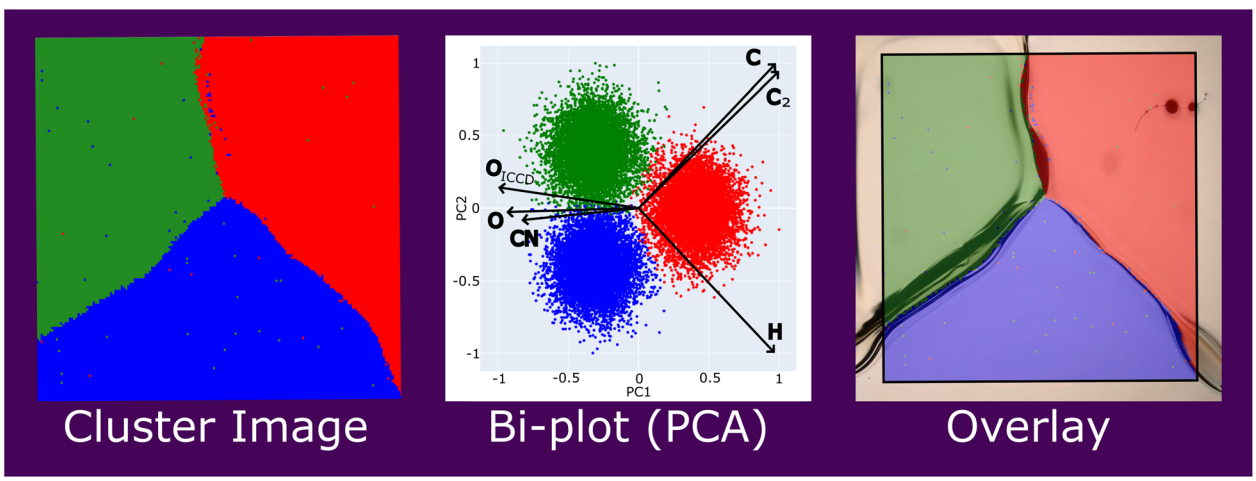

Fig. 4 Chemometric evaluation of LIBS data: cluster image (of *k*-means cluster analysis), Bi-plot of a PCA and overlay of cluster image with microscopic image. PI is depicted in green, PS in red and PVP in blue.

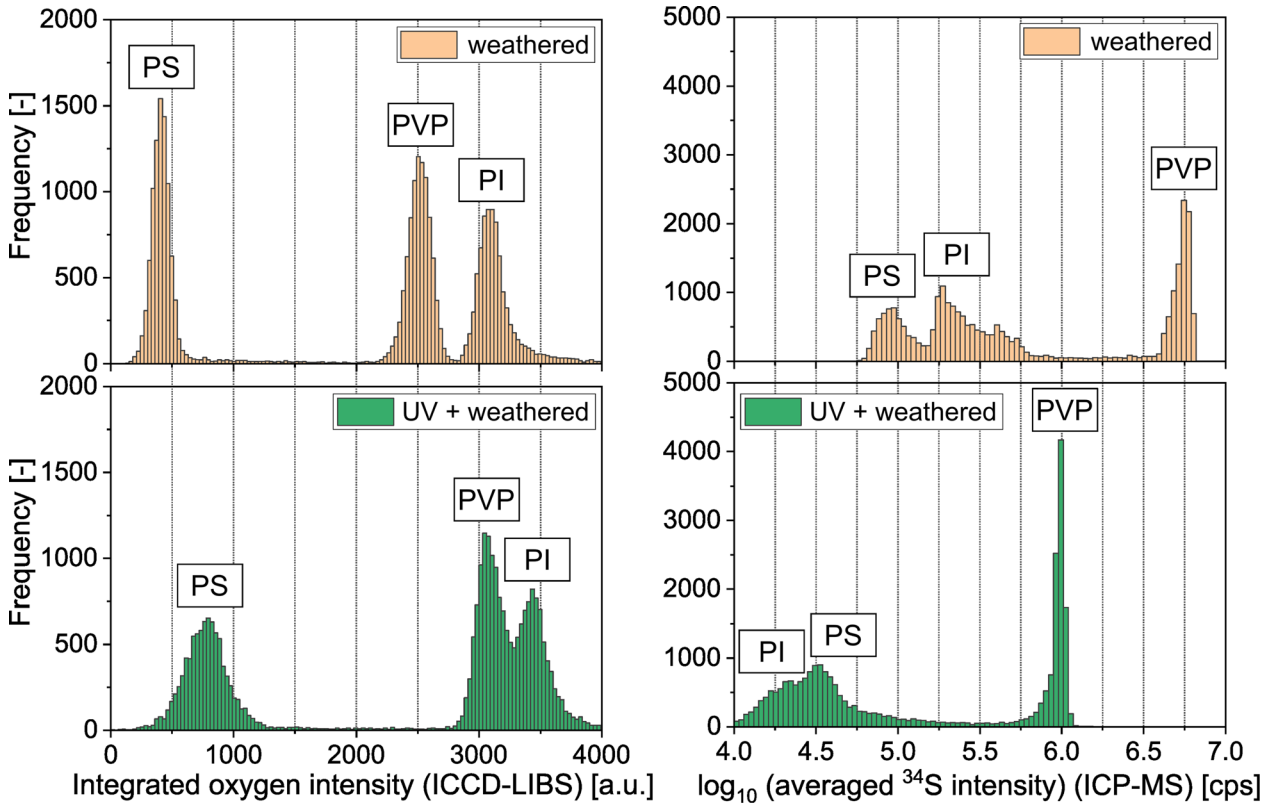

Fig. 5 Histograms for the O signal of ICCD-LIBS (bin size = 30) and $\log_{10}(^{34}S)$ signal of LA-ICP-MS (bin size = 0.03) of images of H_2S weathered multi-polymer samples with and without prior UV treatment.

UV treated and weathered polymer films are the lowest for PS, significantly higher for PVP, and the highest for PI. The relative ranking is consistent with the amount of oxygen atoms per repetition unit (none in PS, one in PVP and five in PI). For all three polymer types, the oxygen signal intensity distribution of the UV-treated films is shifted to higher signal intensities compared to non-UV-treated films, indicating oxidation through the UV treatment in the ambient atmosphere – a finding which is consistent with published literature.[30,31] In contrast, the ICP-MS data for sulfur indicates that the UV-treated polymers show a significantly lower uptake compared to the non-UV treated films. As can be seen in Fig. 5 for the non-UV treated films, PS shows the lowest, PI slightly higher and PVP the highest sulfur intensities. For the UV treated and weathered polymers, although significantly decreased, PVP still shows the highest intensity for sulfur. For PI the intensity decreased more than for PS through the UV treatment, changing the relative sulfur intensity ranking between the two of them to PI at the lowest and PS to slightly higher sulfur intensities.

The presented qualitative results already show an effect of the UV treatment on the polymer properties. However, since it can be assumed that the ablation rates vary between the polymer types, an adequate comparison between them is not possible. Further, the presented results do not include depth information. To investigate the depth that is affected by the UV-induced changes in the polymer composition, as well as the changes of the sulfur concentration with the sample depth, and to further enable a comprehensive comparison between the polymer types, the following section is dedicated to the optimized analysis of depth profiles and the quantification of the results for sulfur.

3.2.2. Depth profiles. Each depth profile was measured using ten repetitive line scans (8 mm) on the same sample location. Each line scan resulted in one transient ICP-MS signal for each measured isotope with a duration of about 1.5 s, and one LIBS spectra, which was averaged over the 160 single shot spectra recorded per line. The depth profiles were measured at three different locations on each sample with a distance of 500 μm. The data points and error bars in Fig. 6 are calculated from the averages of the three-line scans with the respective sample depth and the standard deviation, respectively. The total crater depths of ten-line scans were determined by profilometer measurements with a "DektakXT" (Bruker, MA, USA) as 1.8 μm for PI, 1.5 μm for PS, and 3.6 μm for PVP. Crater depth measurements showed a linear relationship between the total ablation depth and the number of ablated layers in previous experiments with the 193 nm excimer laser (having a flat-top beam profile), up to a total ablation depth of more than 20 μm. The resulting ablation rate per line scan (*i.e.*, depth resolution) was determined as 180 nm for PI, 150 nm for PS, and 360 nm for PVP. To achieve this high depth resolution, a very low laser fluence was used (1 J cm^{-2}). Consequently, the signal intensities detected with the broadband LIBS spectrometer were

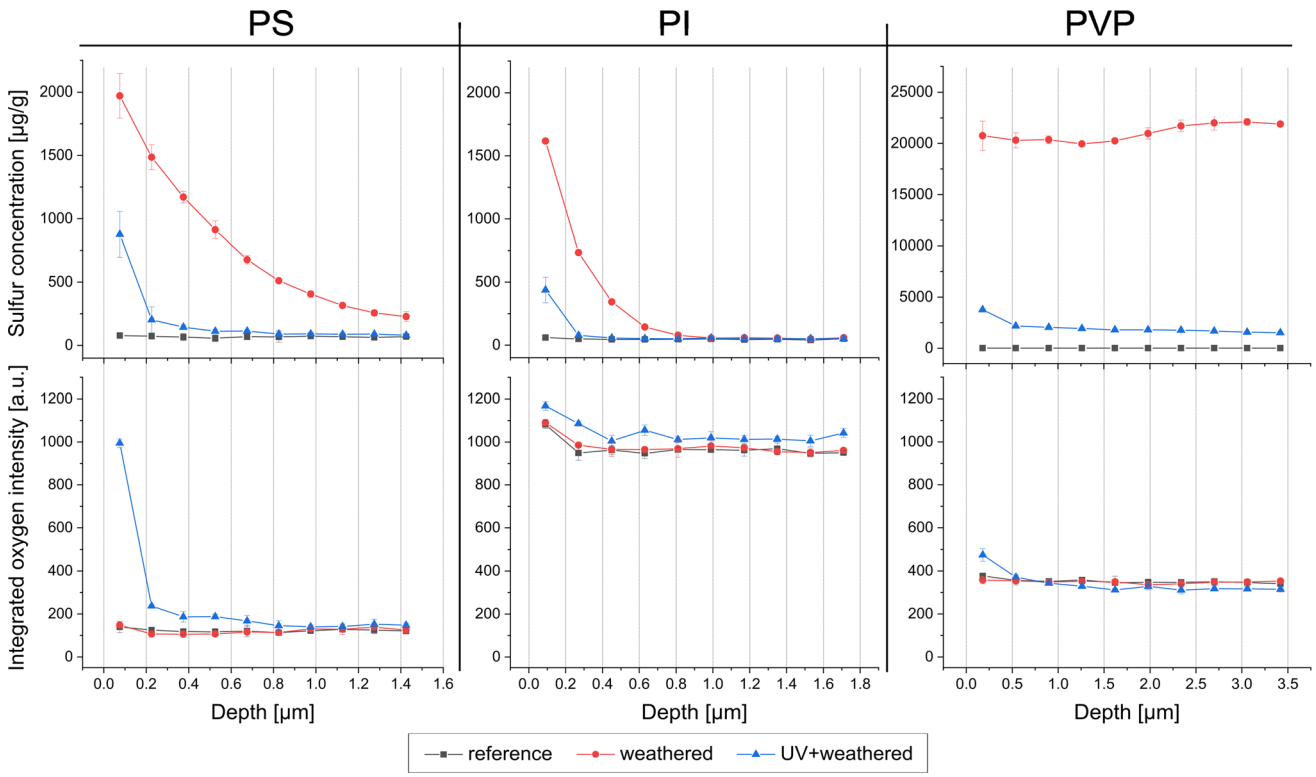

Fig. 6 Simultaneously determined quantitative sulfur depth profiles *via* LA-ICP-MS and qualitative oxygen depth profiles *via* LIBS of PS, PI, and PVP. Of each polymer type, an untreated reference, a UV-treated and subsequently weathered, and a non-UV-treated and subsequently weathered sample film was measured.

insufficient for evaluation. However, with the ICCD detector, acceptable signal-to-noise ratios were detected.

Matrix-matched standards for each polymer type were measured and evaluated using the same parameters as the depth profile measurements. Normalizing the signal to carbon, which represents a marker for the amount of polymer ablated, the calibration functions delivered correlation coefficients of $R^2 \geq 0.99$. Thus, differences in the ablation behavior and the sulfur response between the polymer types can be compensated, enabling quantitative results for sulfur and allowing a comparison between the different polymer types. Fig. 6 shows the depth profiles for the three investigated polymer types, simultaneously determining the quantitative amount of sulfur *via* LA-ICP-MS (top) and qualitatively determining oxygen *via* LIBS (bottom). Each plot shows results for an untreated polymer film serving as a reference, UV-treated and subsequently weathered sample, and a non-UV-treated and subsequently weathered sample. The unweathered reference samples do not show any uptake of sulfur. Therefore, the depth profiles show a constant level representing the bulk concentration of the used materials at approximately 70 µg g^{-1} for PS, 50 µg g^{-1} for PI, and 10 µg g^{-1} for PVP. In contrast, significantly increased sulfur concentrations were measured in the H_2S weathered polymer films, showing a different uptake behavior in the different polymer types and between UV treated and non-UV treated polymer films. The non-UV-treated samples show a sulfur concentration of approximately 2.0 mg g^{-1} for PS and 1.6 mg g^{-1} for PI in the first ablated layer. In PS, the sulfur concentration decreases only gradually with the sample depth, showing still slightly more than 200 µg g^{-1} at the maximum measured sample depth of 1.5 µm. In contrast, in PI, the sulfur concentration is reduced to the blank level at a depth of 1 µm. This indicates a higher diffusion rate of H_2S in PS than in PI. Even higher diffusion of H_2S is observed into PVP, showing a sulfur concentration of about 20 mg g^{-1} distributed nearly constant from the surface to a depth of around 3.5 µm. The determined sulfur concentration in PVP exceeds the calibrated range (0.02–5 mg g^{-1}) and is therefore considered a reasonable estimate of the true concentration. It can be observed that the uptake of sulfur is significantly reduced in the UV-treated samples of all investigated polymer types. The surface of PS and PI shows increased sulfur levels of approximately 800 µg g^{-1} and 400 µg g^{-1}, respectively, quickly approaching to the blank sulfur concentration with increasing sample depth. For PVP, the sulfur uptake in the UV treated sample is reduced to 1.5–2.0 mg g^{-1}, which refers approximately to factor of 10. In summary, the results demonstrate that PI shows the best performance regarding the application as a barrier coating in the tested exposure conditions and that UV treatment had a significant positive effect on the barrier characteristics of all investigated polymer types.

As can be seen in Fig. 6 for each polymer type, the oxygen signals of the non-UV-treated and subsequently weathered polymers are not significantly different from the untreated

references. Therefore, the differences to the UV-treated samples can be assigned solely to the UV treatment, excluding effects of the weathering onto the observed oxygen signal intensities (*e.g.*, uptake of water, uptake or loss of oxygen by potentially occurring chemical reaction). For PS, a strongly increased oxygen signal could be measured at the uppermost surface layer, and slightly increased levels down to a depth of 1 μm were observed. Below a depth of 1 μm, no oxidation could be determined. UV-treated PI shows only slightly increased oxygen intensities down to the total measured depth of 1.8 μm. PVP is not significantly different from the non-UV-treated sample, except for a considerably increased oxygen intensity in the uppermost layer. The extent of oxidation and the affected depth show a substantial variation between the investigated polymer types.

The results in this section could identify the affected sample depth of UV-induced polymer oxidation for the investigated polymer types and demonstrate the different diffusion behavior of H_2S and the influence of the UV treatment on the diffusion behavior.

4. Conclusion

This work showed the development of a simultaneous LA-ICP-MS & LIBS setup using a 193 nm excimer laser ablation combined with a single quadrupole ICP-MS, a broadband multichannel LIBS spectrometer, and a high-resolution LIBS spectrometer with an ICCD detector. The setup and measurement procedure were optimized in two ways: (i) – maximal lateral resolution with sufficient signal-to-noise ratio using single-shot LIBS spectra for evaluation and (ii) – maximum depth resolution using repetitive line scans and averaged LIBS spectra. The methods were applied to investigate the properties of thin films of three different polymer types regarding their behavior in degradative treatment and weathering with H_2S.

Analyzing a structured sample that contained all three polymer types, a desired polymer discrimination result could be achieved with a spatial resolution of 40 μm and chemometric evaluation of single-shot spectra, paving the way for creating a reference database and performing classification. This can be very beneficial for questions where the identification of polymer materials is required (*e.g.*, plastic waste separation and recycling, environmental analytics, microplastics research) and the sample amount or size is limited (*e.g.*, thin films, layered systems, micro structured samples, *etc.*). While the investigated polymer types are known in this work, mentioned applications for polymer analysis may lack that information. In such cases, the developed method could be applied for polymer identification. Moreover, knowledge of the polymer type enables the possibility of preparing or purchasing matrix-matched standards for subsequent quantitative LA-ICP-MS, *e.g.*, analysis of elemental contents in quality control required to meet production specification or accumulation or dissipation of substances from or into the environment.

Qualitative data from the ICP-MS and the ICCD-LIBS showed differences in the sulfur uptake between the weathered polymer types and changes to the previously UV-treated samples regarding oxidation and sulfur uptake. Calibration of the ICP-MS using matrix-matched polymer standards with different spike levels enabled quantitative results for sulfur in the measured depth profiles. By compensation of matrix effects in ablation, particle transport, and ionization, this further enabled the comparison of the different polymer types to each other. The depth-resolved results revealed varying degrees of oxidation derived from the UV exposure and that the photo-induced oxidation is mainly observed at the uppermost sample surface. Different H_2S diffusion profiles could be detected, and it was observed that the UV treatment significantly decreased the uptake of H_2S in all of the investigated polymer types. The achieved sensitivity combined with high spatial resolution of 40 μm laterally and ranging from 150–360 nm in depth represent a substantial improvement compared to existing literature (100 μm laterally, 3.3–6.7 μm in depth),[31] enabling an adequate analysis of thin polymer films in regard to the explored research question. The developed measurement methods combined with the testing equipment for sample exposure to controlled environmental conditions pose excellent tools to investigate the properties and degradation of polymer materials and coatings.

Data availability

Data will be made available on request.

Conflicts of interest

The authors declare that they have no conflicts of interest.

Acknowledgements

iRel40 is a European co-funded innovation project that has been granted by the ECSEL Joint Undertaking (JU) under grant agreement No. 876659. The funding of the project comes from the Horizon 2020 research programme and participating countries. National funding is provided by Germany, including the Free States of Saxony and Thuringia, Austria, Belgium, Finland, France, Italy, the Netherlands, Slovakia, Spain, Sweden and Turkey. The document reflects only the authors' view and the JU is not responsible for any use that may be made of the information it contains. The authors gratefully acknowledge the funding by the Austrian Research Promotion Agency (FFG, Project No. 877531 and 877540) and the TU Wien Bibliothek for financial support through its Open Access Funding Program.

References

1 H. Sasajima, I. Watanabe, M. Takamoto, K. Dakede, S. Itoh, Y. Nishitani, J. Tabei and T. Mori, *Materials for Advanced Packaging*, Springer International Publishing, Cham, 2017.
2 J. J. Licari, *Coat. Mater. Electron. Appl.*, 2003, 1–63.
3 C. P. Wong, *Electron. Appl.*, 2005, 63–83.
4 H. Ren, G. Zou, Q. Jia, Z. Deng, C. Du, W. Wang and L. Liu, *Microelectron. Reliab.*, 2021, **127**, 114379.
5 G. Maier, *Prog. Polym. Sci.*, 2001, **26**, 3–65.
6 S. Marano, E. Laudadio, C. Minnelli and P. Stipa, *Polymers*, 2022, **14**(8), 1626.

7 A. Kausar, *J. Plast. Film Sheeting*, 2020, **36**, 94–112.
8 A. Trentin, A. Pakseresht, A. Duran, Y. Castro and D. Galusek, *Polymers*, 2022, **14**, 1–28.
9 S. H. Hamid, *Handbook of Polymer Degradation*, CRC Press, 2000.
10 C. Decker, *Polym. Int.*, 1998, **45**, 133–141.
11 C. Mendes-Felipe, J. Oliveira, I. Etxebarria, J. L. Vilas-Vilela and S. Lanceros-Mendez, *Adv. Mater. Technol.*, 2019, **4**, 1800618.
12 R. Lenz, K. Enders, C. A. Stedmon, D. M. A. Mackenzie and T. Gissel, *Mar. Pollut. Bull.*, 2015, **100**, 82–91.
13 N. J. Everall, *An Introduction to Laser Spectroscopy*, eds. D. L. Andrews and A. A. Demidov, Springer US, Boston, MA, 1995, pp. 115–131.
14 C. A. Wilkie, *Polym. Degrad. Stab.*, 1999, **66**, 301–306.
15 C. Puglisi, F. Samperi, S. Carroccio and G. Montaudo, *Macromolecules*, 1999, **32**, 8821–8828.
16 G. Montaudo, F. Samperi and M. S. Montaudo, *Prog. Polym. Sci.*, 2006, **31**, 277–357.
17 Z. Gajarska, L. Brunnbauer, H. Lohninger and A. Limbeck, *Anal. Bioanal. Chem.*, 2021, **413**, 6581–6594.
18 S. J. Mousavi, M. Hemati Farsani, S. M. R. Darbani, A. Mousaviazar, M. Soltanolkotabi and A. Eslami Majd, *Appl. Phys. B: Lasers Opt.*, 2016, **122**, 1–16.
19 I. Chamradová, P. Pořízka and J. Kaiser, *Polym. Test.*, 2021, **96**, 107079.
20 C. Sommer, J. Nguyen, T. Menzel, J. A. Prume, H. Ruckdäschel and M. Koch, *Polym. Test.*, 2022, **112**, 107623.
21 M. Bonta and A. Limbeck, *J. Anal. At. Spectrom.*, 2018, **33**, 1631–1637.
22 M. Dong, D. Oropeza, J. Chirinos, J. J. González, J. Lu, X. Mao and R. E. Russo, *Spectrochim. Acta, Part B*, 2015, **109**, 44–50.
23 M. Guitreau, J. J. Gonzalez, S. B. Mukasa and M. T. Colucci, *AGUFM*, 2013, **2013**, V53B–V2785.
24 M. Dong, L. Wei, J. J. González, D. Oropeza, J. Chirinos, X. Mao, J. Lu and R. E. Russo, *Anal. Chem.*, 2020, **92**, 7003–7010.
25 L. Brunnbauer, M. Mayr, S. Larisegger, M. Nelhiebel, L. Pagnin, R. Wiesinger, M. Schreiner and A. Limbeck, *Sci. Rep.*, 2020, **10**, 1–10.
26 B. T. Manard, V. C. Bradley, C. R. Hexel, P. Doyle, N. A. Zirakparvar and R. Dunlap, *J. Anal. At. Spectrom.*, 2023, 9–13.
27 B. T. Manard, C. J. Hintz, C. D. Quarles, W. Burns, N. A. Zirakparvar, D. R. Dunlap, T. Beiswenger, A. M. Cruz-Uribe, J. A. Petrus and C. R. Hexel, *Metallomics*, 2022, **14**(7), mfac050.
28 K. Liu, D. Tian, C. Li, Y. Li, G. Yang and Y. Ding, *Trends Anal. Chem.*, 2019, **110**, 327–334.
29 L. Brunnbauer, S. Larisegger, H. Lohninger, M. Nelhiebel and A. Limbeck, *Talanta*, 2020, **209**, 120572.
30 M. C. Celina, *Polym. Degrad. Stab.*, 2013, **98**, 2419–2429.
31 L. Brunnbauer, M. Mayr, S. Larisegger, M. Nelhiebel, L. Pagnin, R. Wiesinger, M. Schreiner and A. Limbeck, *Sci. Rep.*, 2020, **10**, 1–10.